

# International Conference on Space Optics—ICSO 2022

Dubrovnik, Croatia

3–7 October 2022

*Edited by Kyriaki Minoglou, Nikos Karafolas, and Bruno Cugny,*



***A passively heat-sunk 6-W 1064-nm linearly-polarized fiber amplifier with a 100 °C operational temperature range for LEO satellite optical communications***



# A passively heat-sunk 6-W 1064-nm linearly-polarized fiber amplifier with a 100 °C operational temperature range for LEO satellite optical communications

François Gonthier, Viorel Poenariu, Sean McCarthy, Qi Yang Peng, Daoping Wei, Vincent Latendresse, MPB Communications Inc., 147 Hymus Boulevard, Pointe-Claire, Quebec, Canada, H9R 1E9

## ABSTRACT

A 6 W fiber optic amplifier at 1064 nm has been designed for LEO satellites. The amplifier is passively cooled and operational for a heat sink plate temperature from -35°C to +65°C. It is polarization-maintaining and is designed for a 2.7 Gbps phase-modulated single-frequency (10 kHz) signal at 1064 nm with an input power between 1 and 20 mW. The unit has a set of redundant pump laser diodes and redundant photodiodes (PD) as well as redundant inputs ports but does not contain any electronics and power supply which are provided externally. A qualification module was tested from -35°C to +65°C and when though, vibration and shock, and electro-magnetic testing. The unit showed good performance except for the extreme temperatures where the maximum power output of 6 W was not achieved because of the specified current limit. An increase in the current of 4% at +65°C and 17% at -35°C was required to reach 6W. The operational 5W specification was achieved at all temperatures. Furthermore, the module was submitted to a 25 krad accelerated non-operational radiation test to measure the effect of photodarkening. A post radiation photobleaching was performed to better estimate the degradation in space during operations. The experimentally estimated loss from the predicted 8 krad exposition during the lifetime of the units is 3%. Four flight modules were built and tested in the operational temperature range of between -30 °C and +60°C as well as in vibration.

**Keywords:** 1064 nm fiber amplifier, passively cooled, wide temperature range, space fiber amplifier, LEO satellites, space laser communications,

## 1. INTRODUCTION

Laser space communications<sup>1</sup> has seen a significant number of commercial systems in recent years<sup>2</sup>, despite the difficult environment and satellite requirements. One of those common constraints pertains to temperature control. Optical fiber amplifiers in LEO satellites are usually temperature regulated by coupling them to a radiative heat sink. This still results in large temperature variation as the satellites circle the Earth every 90 minutes or so. Though many systems manage the temperature range around 60 °C, we present here a 6W 1064 nm fiber amplifier that operates over a range of 90°C<sup>3</sup>.

The extended temperature results into larger wavelength shifts in the pumps wavelengths and changes in the pump and fiber efficiency. Furthermore, the high-power operation also brings its challenges with high dissipation and non-linear effects in the fiber such as Stimulated Brillouin Scattering (SBS). Finally, the system requirements add other limits such as size and weight, as well as driving currents. A further requirement was to use telecom grade components rather than space qualified parts. To address these constraints, after several breadboard experiments and component qualifications, a qualification model was made and thoroughly tested in a thermal vacuum chamber and for vibration and shock and finally radiation exposure. Four (4) Flight modules were subsequently built.

In this paper, we will first summarize the systems requirement, explain the amplifier design, show the qualification module performances and test results, and finally present the flight modules results.

## 2. SYSTEM REQUIREMENTS

A summary of the systems requirements for the amplifier is presented in Table 1.

Table 1. System requirement summary

Parameter	Min	Nom	Max	Unit	Condition
<b>Optical requirements</b>					
Wavelength		1064		Nm	
Input power	1		20	mW	
Optical input linewidth		10		kHz	
Signal characteristics 1: Phase modulation		2.7		Gbps	BPSK signal 2 <sup>7</sup> -1pseudo random sequence
Signal characteristics 2: Phase and Amplitude modulation	1		2	MHz	0% to 100%
Maximum optical output	6.0			W	Average optical power
Operational optical power	5.0			W	Average optical power, must be met in all conditions at end of life
Polarization state					Linear polarization; along the slow axis
Output polarization extinction ratio			-20	dB	
Tolerable Back Reflection	-40			dB	
Residual power at output			-40	dB	
Signal-to ASE power ratio	33			dB	At 5W output power. Measured in a 1 nm interval at the footprint of the amplifier signal
Total ASE			50	mW	
Noise Figure			10	dB	
<b>Amplifier design requirements</b>					
Number of stages		3			
Monitoring: input power, output at every stage, back reflection for stage 2 and 3					all with second monitor in cold redundancy
Temperature monitoring, thermistors		2			
Pump lasers for every stage					second set in cold redundancy
Redundant input fibers					
Output fiber length		4		m	
Unit size:	24,6 x15,6 x 6,5			cm	
Unit weight	1540	1580	1620	g	
<b>Electrical requirements</b>					
Overall power consumption			33	W	
First stage pump current	0,25	0,3	0,35	A	
Second stage pump current	2,0	3,1	3,2	A	
Third stage pump current	4,3	4,8	5,3	A	
<b>Environmental requirements</b>					
Acceptance temperature range	-30 °C to +60 °C				
Qualification temperature range	-35 °C to +65 °C				
Vacuum		10 <sup>-5</sup>			hPa

Other requirements not listed in Table 1 are the vibration, shock, and EMC, which the units passed but will not be discussed in this paper. The radiation requirement will be discussed in Section 4.

The items above are the main requirements that influenced the design.

### 3. DESIGN

This amplifier is 3-stage design with cold redundancy on all the optoelectronic elements and has 2 parallel input ports. The amplifier use polarization maintaining fiber for the signal path as well as polarization maintaining components. The isolators are single-polarization and act as polarizers to help achieve the 20 dB Polarization Extinction Ratio (PER) specification. The amplifier was divided in 3 stages that are presented in Figures 1, 2 and 3 for stage 1, 2 and 3 respectively. The 3-stage design was selected to provide better stability of the systems over the operating conditions.

The input fiber is a PM980 fiber. The first stage uses a single-mode, single-clad Yb-doped gain fiber pump with 1 976 nm grating stabilized laser diode (LD) with a maximum of 460 mW output (LD1). It is combined with another pump (LD6) in cold redundancy with a polarization combiner (C6) before being combined with the signal in the gain fiber by WDM coupler W1. One purpose of the first stage is to compensate the intrinsic loss at the input caused by the 50% coupler C1 which combines the 2 redundant input ports with 3 dB loss and the input isolator I1 insertion loss. At the output of the gain fiber, an isolator I2 protects the first stage from back propagating light (back-reflection of Amplified Spontaneous Emission (ASE)) and a 2% tap coupler that allows both the measurement of the stage 1 output and the stage 2 backward signal.

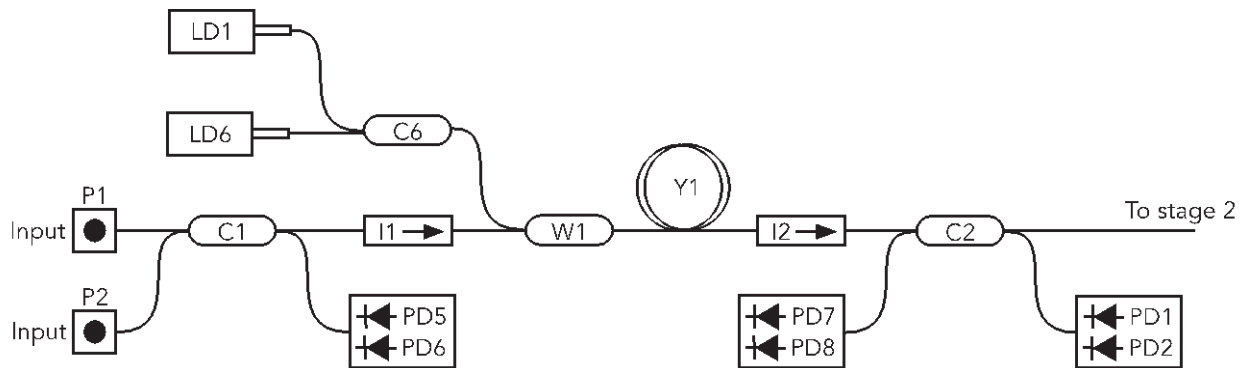


Figure 1. First stage optical schematics with redundant input ports P1 and P2, input monitor (PD5 and PD6), single-mode 976 pumps (LD1 And LD6), isolators I1 and I2, gain fiber Y1, Stage 2 back-reflection monitor (PD7 and PD8) and stage 1 output monitors (PD1 and PD2)

The second stage uses a Double-Clad Fiber (DCF) Yb-doped fiber with a 10  $\mu\text{m}$  core as the gain medium. It is pumped with a 915 nm 10W multimode laser diode (LD2) that is combined, as is its redundant counterpart (LD7) via a (2+1) x 1 combiner. The 7.85 m gain fiber is specially spooled to a diameter to obtain a good PER performance. As for the first stage, it is protected at the output by a high power (2W) isolator and has a 2% tap coupler for monitoring co- and counter-propagating light.

The third stage is pumped by three (3) 915 nm 10W multimode laser diode (LD3 to LD5) to provide the high-power output. The nominal pumps, as well as the redundant pumps (LD8 to LD10) are coupled to the DCF 10  $\mu\text{m}$  Yb-doped gain fiber with a (6+1) x1 combiner. The output power is monitored with an inline -45dB redundant monitor. Because of its bulk and optical loss, an output isolator is not used. This makes it sensitive to back-reflections. Thus, the output back-reflection and Stimulated Brillouin Scattering (SBS) have been thoroughly tested and monitored. Since the output fiber is 4 m, the last stage gain fiber was shorter (4.5 m) than the second stage fiber. It is spooled in the same manner. The fiber routing after the gain fiber was kept to a minimum inside the unit.

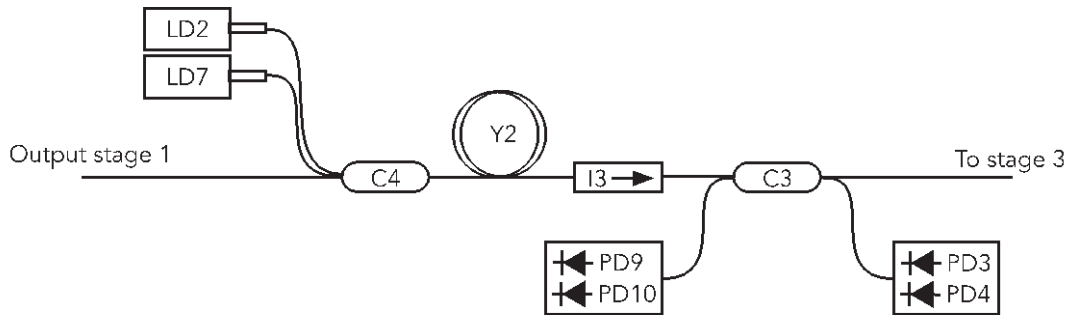


Figure 2. Second stage optical schematics with 2 multimode 915 nm pumps (LD2 and LD7), a (2+1) x 1 combiner C4, the gain fiber Y2, Stage 3 back-reflection monitor (PD9 and PD10) and stage 2 output monitors (PD3 and PD4).

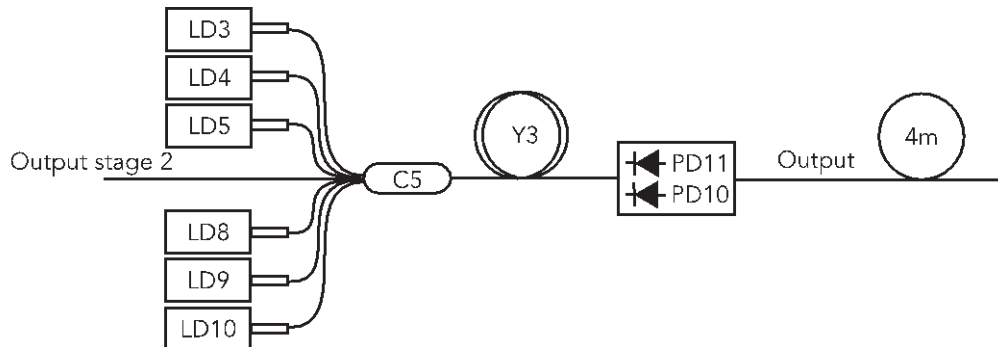


Figure 3. Third stage optical schematics with 6 multimode 915 nm pumps (LD3, LD4, LD5 and redundant LD8, LD9 and LD10), a (6+1) x 1 combiner C5, the gain fiber Y3, an inline output monitors (PD11 and PD12) and 4 m of output fiber.

The unit does not contain laser drivers or power supplies, or any control electronics. This is provided externally by 2 redundant connectors that can both access the nominal and redundant opto-electronics. The nominal and redundant optoelectronics are fully tested in the units, both on the qualification and flight modules and show some performance differences. A unit is acceptable if the worst performing path passes.

#### 4. QUALIFICATION MODULE

Before building the qualification module, all the optical and optoelectronic components required to build the module had to be selected for space use. All the components had already a Telcordia level qualifications. No parts designed specifically for space were used. Extra thermal vacuum (TVAC) testing, including month long operation for the pump diodes, have been performed as well as severe vibration and shock tests. The components were also tested for radiation. For the gain fibers, no rad-hard fibers are used, but the best radiation tolerant fibers were selected<sup>4,5</sup>. Hence, some degradation is expected in the lifetime and the qualification module help estimate this effect.

Thus, to validate the design and qualified it for the space environment, a qualification module was built and passed the following test sequence (Figure 4). The sequence includes tests and measurements during integration, to calibrate all the monitoring photodiodes and characterize the output power of each stage of the amplifier. The functional measurements performed at each temperature include the operation data at 5 W and 6W, residual pump power, signal to ASE ratio, and noise figure. Other measurements such as SBS and PER were not performed in the TVAC chamber because of the output feedthrough which influence the measurement. Vibration and Shock, EMC and radiation were performed at other facilities in atmospheric conditions. The results were reviewed by a technical review board (TRB) before the unit was accepted.

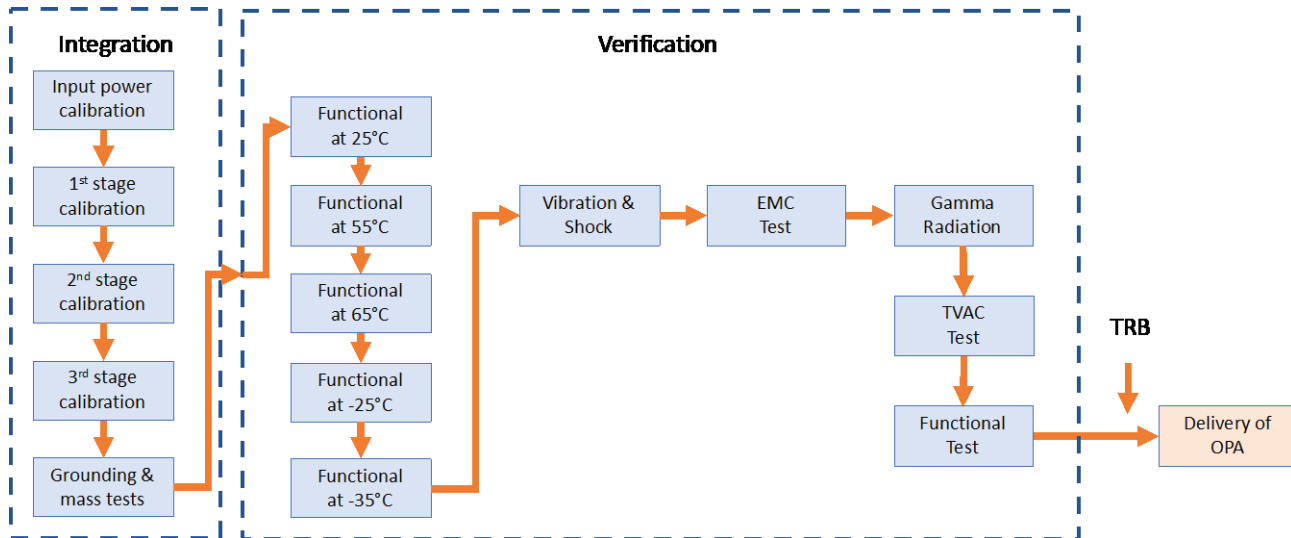


Figure 4. Qualification module integration and verification sequence.

#### 4.1 TVAC tests

The TVAC tests were performed in the vacuum better than  $10^{-5}$  Torr. The unit was stabilized for at least 1 hour on the chamber's cold plate at each temperature before all the tests at this temperature were performed. The  $-35^{\circ}\text{C}$  and  $+65^{\circ}\text{C}$  correspond to the qualification temperature. The  $-25^{\circ}\text{C}$  and  $+55^{\circ}\text{C}$  correspond to the operational temperatures. The  $25^{\circ}\text{C}$  in Figure 4 actually stands for room temperature, which was more precisely  $22.5^{\circ}\text{C}$ . For all the operational test presented below, the current of the first stage was set to 350 mA, which translated to about 220 mW for the first stage pump power at room temperature, and the current of the second stage was set to 3.1 A, which translated to about 2.6 W for the second stage pump power at room temperature. Only the third stage current was changed during the measurements.

Though the tests were done sequentially at each temperature they are summarized by tables for all the temperatures to visualize the temperature dependences.

The functional tests started with the operating current for 5 W and the power consumption. The third stage currents and the power consumption are shown in Figure 5 for both the nominal and redundant pumps as a function of temperature. The input power was 20 mW in P1 input port; the narrow linewidth source wavelength was 1064.5 nm. It is clear that the unit's performance is optimum at room temperature and degrades toward the extreme temperatures, as expected. The degradation at high temperature is due to a lower electrical to optical efficiency of the pump laser diodes. At cold temperature, the diodes are more efficient, but their wavelength shift to 895 nm, reducing the amount of pump that is absorbed in the third stage gain fiber. At  $-35^{\circ}\text{C}$ , the drive current of the third stage is very close to the maximum, but the power consumption is above the 33 W requirement. The unit is fine at  $-25^{\circ}\text{C}$ . The failure at  $-35^{\circ}\text{C}$  of the QM was not considered a major problem because of a simple solution could be applicable to the FM units. To improve the performance, the pump power of the third stage could be increased by selecting a better combiner. The one in the QM unit had an average of 91% coupling. The combiners in the flight unit have coupling efficiency of 95%.

The temperature effect on the pumps is also when the amplifier is operated at 6 W output power. Figure 6 shows the third stage current for a 6 W output for the nominal and redundant pumps for 1 mW and 20 mW of input powers. This figure shows that the input power does not matter for the output confirming that the amplifier output is saturated. It also shows the same good performance at room temperature and the degradation going to the extreme temperatures. Though the output can reach 6 W, the third stage current is above the current limit requirement at  $+65^{\circ}\text{C}$  and at  $-25^{\circ}\text{C}$  and below. The explanation is the same as for the 5 W output results and the solution to improve is also similar, that is to improve the efficiency of the third stage combiner.

The temperature shift on the pump can clearly be seen in the residual pump power. The amplifier output spectra are shown in Figure 7 at the different temperatures. The figure also shows that the residual pump is more than 50 dB below the maximum signal, meeting the requirement of 40 dB.

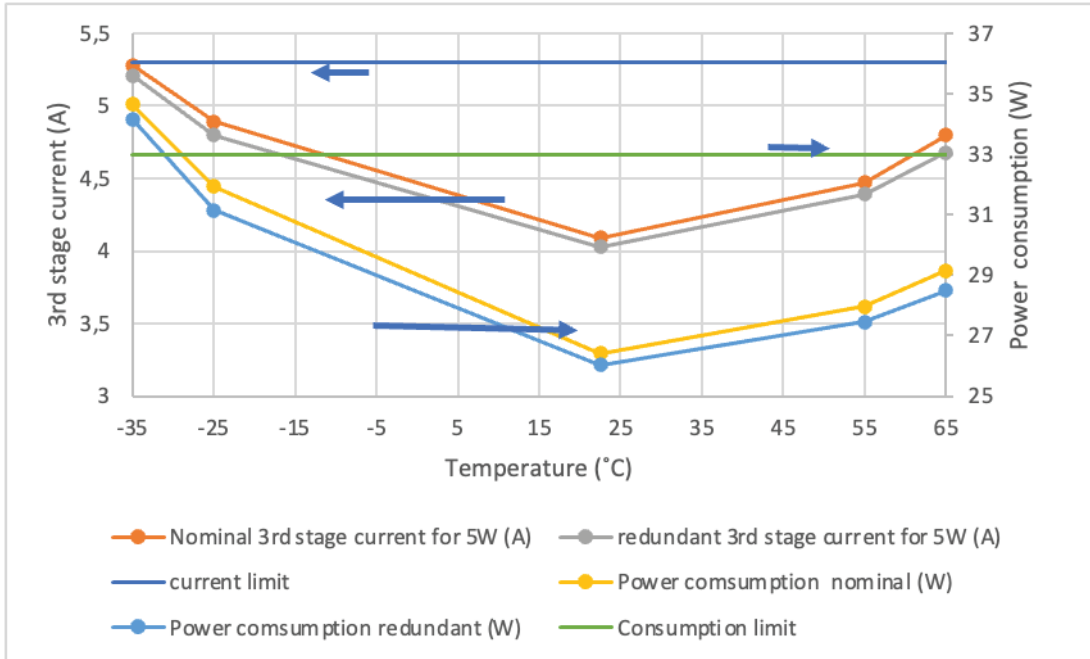


Figure 5. Qualification module 5 W operation and power consumption in vacuum.

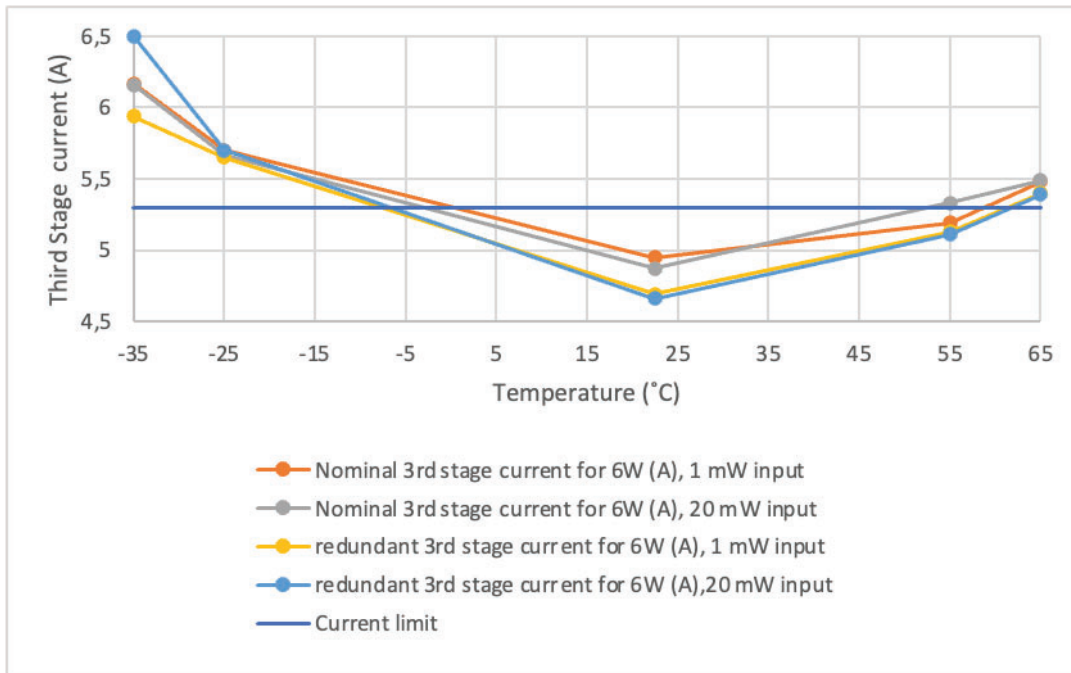


Figure 6. Third stage current for the nominal and redundant pumps, for a 6 W output power in vacuum.

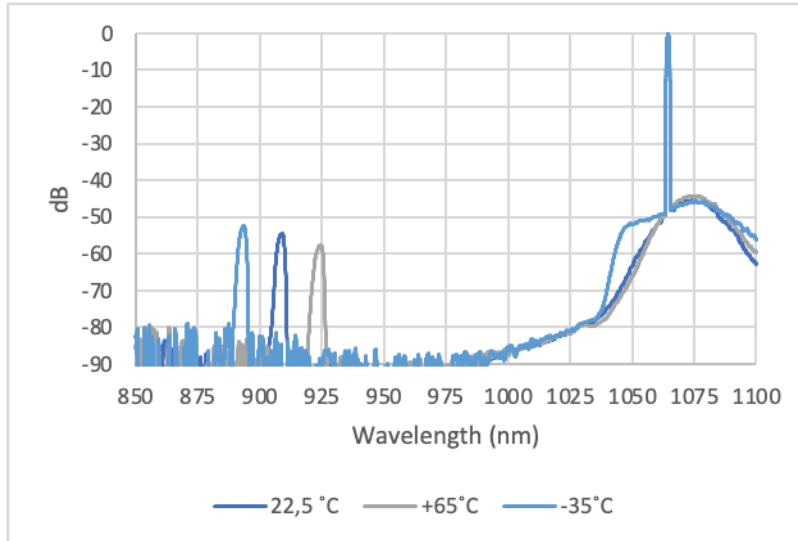


Figure 7. Output spectra showing residual pump power for 3 different temperatures for a 20 mW input and 6 W output powers. All spectra have been normalized to a 0 dB maximum.

The spectra in Figure 7 also show that the ASE ratio is not significantly affected by temperature. The signal to ASE ratio is summarized in Table 2 and is always greater than 33 dB. The total ASE remains small.

Table 2. Signal to ASE ratio and total ASE for different temperatures for a 20 mW input and 5 W output.

Temperature (°C)	Signal to ASE ratio (dB)	Total ASE (mW)
-35 °C	47,34	2,9
-25 °C	47	2,3
22,5 °C	46,63	2,5
55 °C	43,24	5,2
65 °C	44,17	3,4

The last parameter measured at different temperature is the noise figure, which remained between 7 and 9.5 dB, better than the 10 dB requirement.

#### 4.2 Tests at room temperature

The following measurements were performed with the TVAC chamber open, without the feedthrough, as it can influence the measurements. In particular, the SBS threshold strongly depends on the output fiber length and the feedthrough itself add more than 2 m passive fiber. Thus, the SBS was monitored with the third stage back reflection photodiode PD9 (Figure 8). The measurement was taken with both phase and amplitude modulation on the input signal. The back-reflection increase is still approximately linear, showing that the SBS threshold has not been reach at 6 W output.

The PER, measured with a polarized ASE source over 30 minutes was 21 dB, meeting the minimum 20 dB requirement

The Vibration and Shock qualification were performed at laboratory temperature. The vibration tests were typical of the LEO satellite launch with resonance search (5 -2000 Hz, 0.5 G), Random vibration (20 -2000 Hz), sine vibration (5-100 Hz, 25 G). After the vibration test, a micro-vibration test was performed (1 to 1000 Hz, 0.002 to 0.02 G). The shock test was up to 2000 G at 10 kHz. The amplifier was tested before and after each test, and during the micro-vibration test. The micro-vibration test shows no effect on the unit. The operation measurements before and after the mechanical tests show variations of less than 1 % which is within the experimental error, as the unit was connected and disconnected at each test.

The EMC test was also performed at laboratory temperature and unit was not affected.

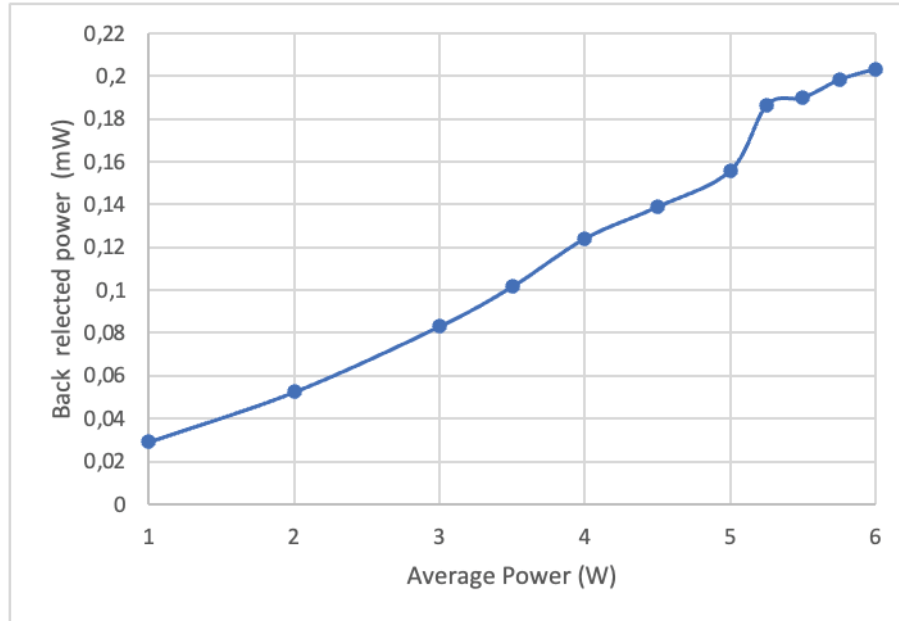


Figure 8. Calibrated back relection measurement (PD9) at room temperature as the amplifier output power is increased to 6 W.

### 4.3 Radiation tests

The QM unit was exposed to a 25 krad dose in a 62-hour period. This dose represents 3 times the expected lifetime dose on the gain fibers. Because, for practical reasons, the dose is applied over a very short period, this photobleaching effect present in a operating amplifier is neglected and the consequence is a very strong loss in the gain fibers by photodarkening. To recover, the amplifier is than operated at high power for photobleaching the gain fibers, to the recover some of the output power. The first photobleaching session was 4 hours for stage 1 and 2 hours for stage 2. Then, the unit was photobleached with normal operating power for 69 hours.

Table 3 summarize the output power before and after 69 hours of photobleaching. For a 5W output, the third stage current has increased 0.55 A or 13%. The power consumption has increased by 2,8 W.

Table 3. Comparison of third stage currents for 5W output, before and after radiation with 69 hours of photobleaching.

$P_{in}$ (mW)	Current 3 <sup>rd</sup> stage pumps After functional test (LFFT8) (A)	Output power (SFFT8)	After radiation and 69 hours photobleaching (LFFT9)	Output power (SFFT9)	Difference in power (W)	Difference in current (A)	Variation in current (%)
1	4.21	5.32	4.76	5.23	-0.09	0.55	13%
20	4.1	5.28	4.6	5.27	0.00	0.5	12%

A longer photobleaching period is required to recover the performance. The unit currents were set at 350 mA first stage, 3,1A second stage and 4,2A third stage. The heat sink was at 22.5°C and the unit was connected directly to the power meter. The input source was an ASE source (1020 to 1080 nm). The data was recorded and shows a 5% additional recovery after 10 days, which brings the radiation-induced efficiency loss to around 8%. The estimate 8 krad dose should thus cause an estimated 3% drop in power. Table 4 estimates the end-of-life current needed to reach 5 W based on a 8 krad dose. Though the amplifier does not still meet the maximum current requirement at -35 °C, it does over the operation temperature range.

Table 4. Estimated current at estimated 8 and 25 krad end-of-life dose at different temperatures

Nominal Third stage current for 5W (A)	-35°C	-25°C	22.5°C	65°C
before radiation	5.3	4.8	4.1	4.8
After radiation (25 krad and 400 hours of photobleaching)	<b>6</b>	<b>5.46</b>	<b>4.6</b>	<b>5.2</b>
Estimated current after an 8 krad dose (Estimated end-of-life without photobleaching)	5.5	5	4.25	4.9

#### 4.4 Qualification module conclusion

The qualification module meets all the requirements expect the power consumption at -35 °C and it does not reach 6 W output power at -25°C and -35°C because the maximum current is limited to 5.3 A. It does achieve the 5 W operational output at those temperature with sufficient margin to cover the estimated radiation degradation of 3% with some room to spare. The poorer performance at cold temperature in due to the wavelength shift of the pump diode to 895 nm, which reduces the amount of absorbed power in the third stage. A simple solution, in the selection of combiners with lower insertion loss for the pump (i.e. 95%) is implemented in the flight modules and procure more pump power for the same current and thus increase the output.

## 5. FLIGHT MODULES

Three flight modules (FMA, FMB, FMC) were built, all containing a lower insertion loss pump combiner for the third stage. A photograph of a completed flight modules is shown in Figure 9.

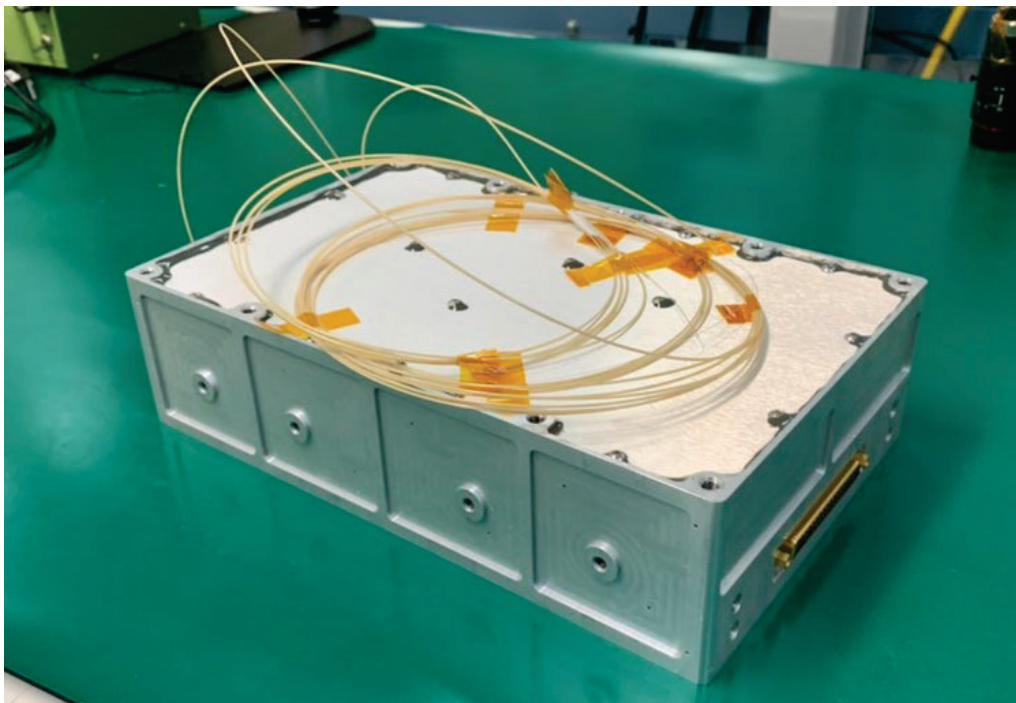


Figure 9. Completed flight module, with 2 input ports and one output port. One electrical connector is shown with a shorting connector. The other electrical connector is on the opposite side of the module.

The testing of the flight module is less demanding than that of the qualification module. The test flow chart is shown in Figure 10. The Long Form Functional Tests (LFFT) perform at all temperature are 5W operation and power consumption, 6W maximum power, ASE measurement, and Noise Figure. The temperature range is reduced compared to the qualification test to -30 °C to 60 °C which is still larger than the operational -25°C to 55°C. An active cycling test is added as well as 8 passive cycles test. The vibration test is done at reduced levels and there is no shock test.

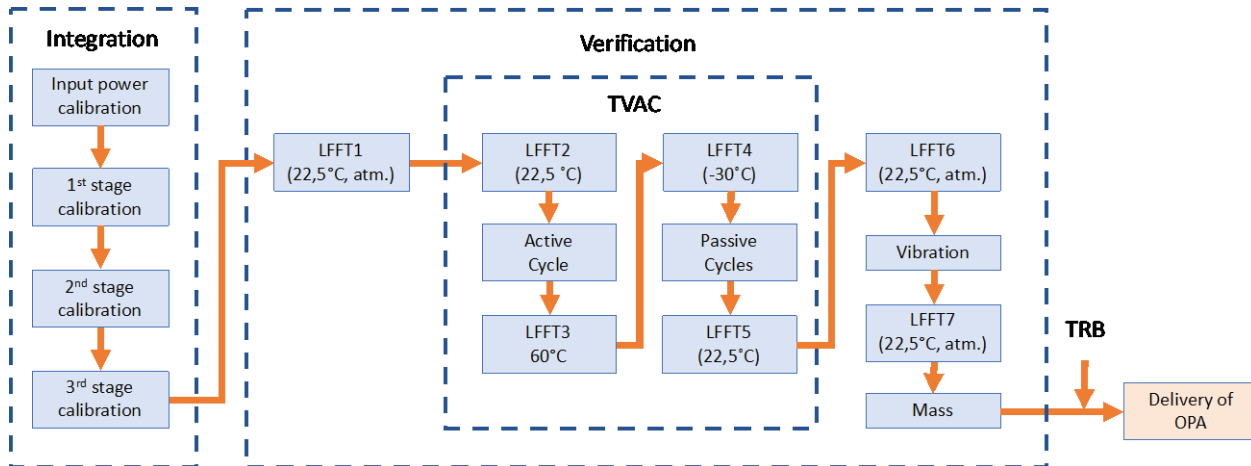


Figure 9. Test flow chart for the flight modules. LFFT stands for Long Form Functional Test.

### 5.1 Improved TVAC performance

The only difference between the QM module and the flight modules is the selection of a lower loss of the third stage combiner. This improves the performance over the whole temperature range. This can clearly be seen in Figures 10 and 11, which show the 5W current and power consumption respectively. The flight modules nominal and redundant (denoted by R) performances are presented. For all the flight unit, the power consumption is below 33 W from -30 °C to 60 °C.

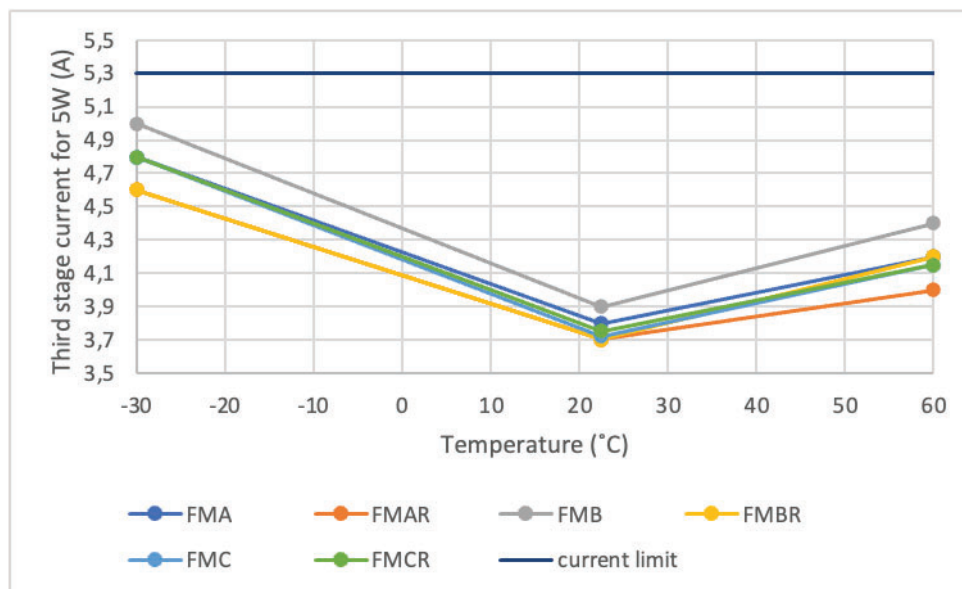


Figure 10. Flight modules third stage currents for 5 W output.

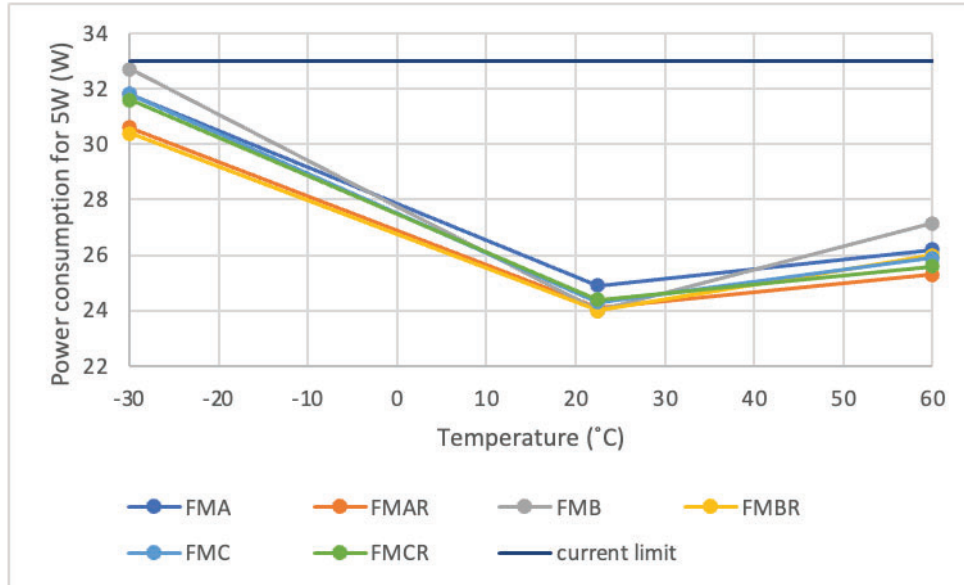


Figure 11. Flight modules power consumption for 5 W output.

The same improvement can be seen in Figure 12 for the third stage current for a 6 W output for the flight modules, though it is not enough to meet the requirement at -30 °C for all the cases. Even if the requirement is not met, the margin of operation is large enough for operating at 5 W, even at end-of-life.

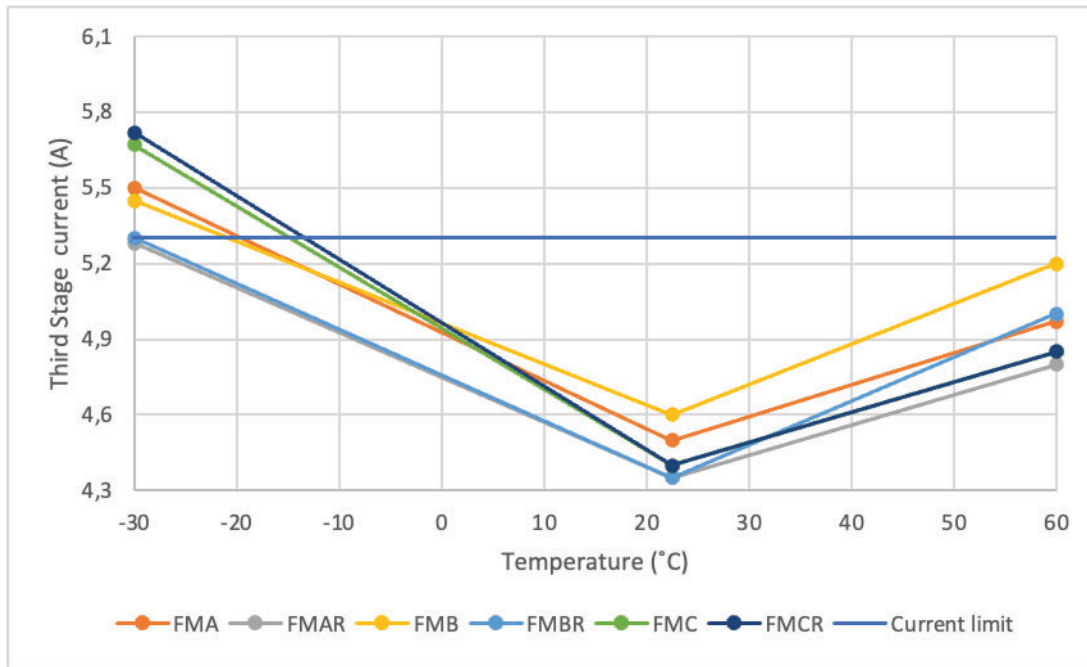


Figure 12. Flight modules third stage currents for 6 W output.

Table 7 give the signal-to-noise ratios and total ASE measured on the optical spectra of the flight modules at the given temperatures. Table 8 gives their noise figures. Neither show a temperature dependence. To detail more of the temperature effect on the amplifier, additional operational results are given in the next section.

Table 7. flight modules signal-to-noise ratio and total ASE.

Temperature (°C)	FMA		FMB		FMC	
	Signal to noise ratio	Total ASE (mW)	Signal to noise ratio	Total ASE (mW)	Signal to noise ratio	Total ASE (mW)
-30	36.7	18.3	38.1	37.3	40.7	15.3
22.5	37.2	17	39.5	11.7	40.8	17.2
60	33.1	83	38.3	14.2	40.4	15.7

Table 6. flight modules noise figures.

Temperature (°C)	FMA	FMB	FMC
-30	8.1	8.7	7.3
22.5	8.1	7.3	7.2
60	8.45	7.35	7.35

## 5.2 Operational temperature results

The amplifier 3 stages use different pumps and/or different fibers and fiber lengths. Each stage behaves differently with temperatures. Figure 13 presents the first stage output power (FMC) as a function of pump current. The input power is 3 mW. The stage is pumped with a 976 nm grating stabilized laser diode. The stage is most efficient at room temperature and loses efficiency at high temperature as would be expected from the loss of efficiency of the single-mode laser diode. However, it is much worse at -30°C. The amplifier barely amplifies the signal. This is caused by the wavelength shift of the laser wavelength that moves toward to lower wavelength and is not stabilized by the Bragg grating anymore. The pump absorption is greatly reduced, but is not zero because some amplification remains, enough to compensate the loss of the input coupler and other components. At higher current, the pump heats up and shift slightly toward the 976 nm absorption peak of the Ytterbium, creating close to a 3 dB gain at 450 mA current.

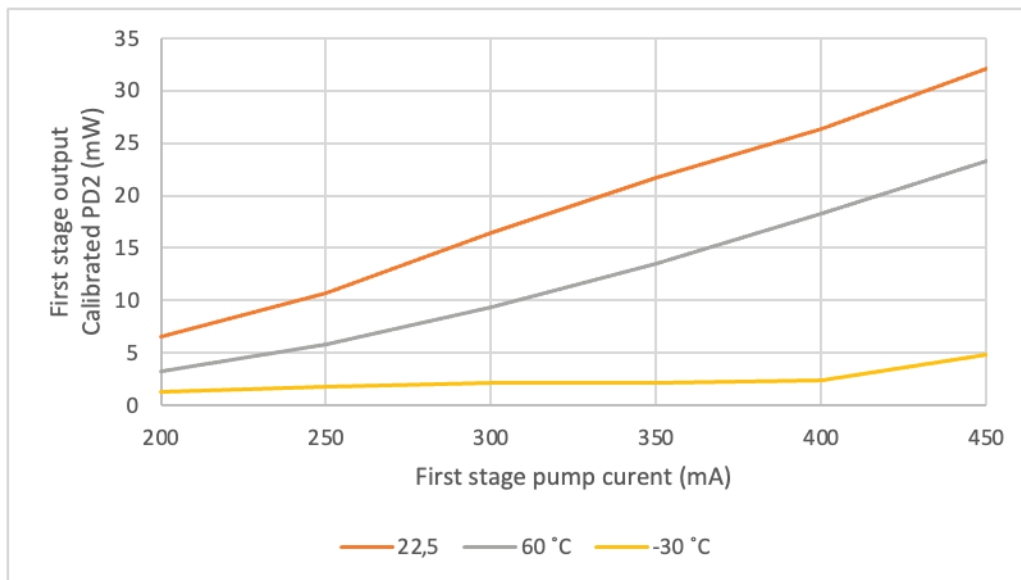


Figure 13. FMC first stage output versus pump current for 3 temperatures

The first stage feeds into the second stage. The second stage is pumped with a 915 nm multimode laser diode that is combined into a 10 µm core DCF fiber. The gain fiber length is 7.85 m. Figure 14 presents the second stage output

power as a function of pump current at 3 temperatures. The first stage is operated at 350 mA. The room temperature performance is the best followed by the -30 °C one. This is even though the first stage output is about 2 mW. As we observed in section 4.1 with the residual pump, the pump wavelength shifts to 895 nm. The absorption is reduced, but not significantly due to the long fiber length. The reduction of the efficiency of the pump at 60°C has a larger effect on the efficiency of the second stage than the temperature shift of the pump at -30 °C. The second stage compensates the first stage lower performance at -30 °C. In all the cases though, the second stage output is several hundreds of milliwatts.

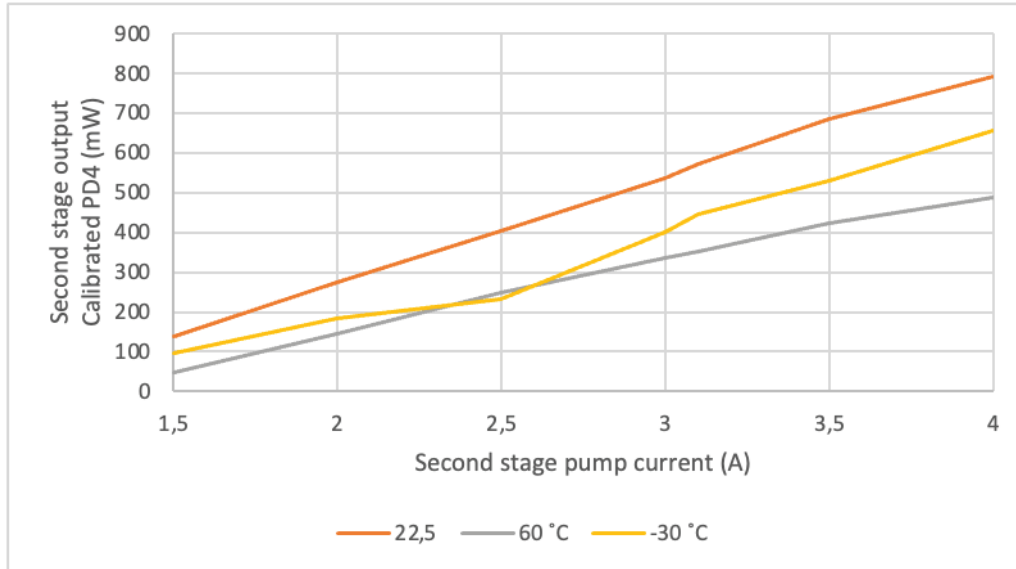


Figure 14. FMC second stage output versus pump current for 3 temperatures. The first stage is operated with a pump current of 350 mA.

The third stage uses the same pumps as the second stage and the same DCF gain fiber, but the fiber length is shorter at 4.5 m. The reduced length was selected to reduce the risk of SBS because of the long output fiber. Here, the most efficient temperature is still 22.5 °C, closely followed by the high temperature. Because the fiber is shorter, the reduced absorption due to the wavelength shift of the pumps at -30 °C has a noticeable impact on the efficiency. The effect of the wavelength shift of the pumps are also clear observed during the active cycle.

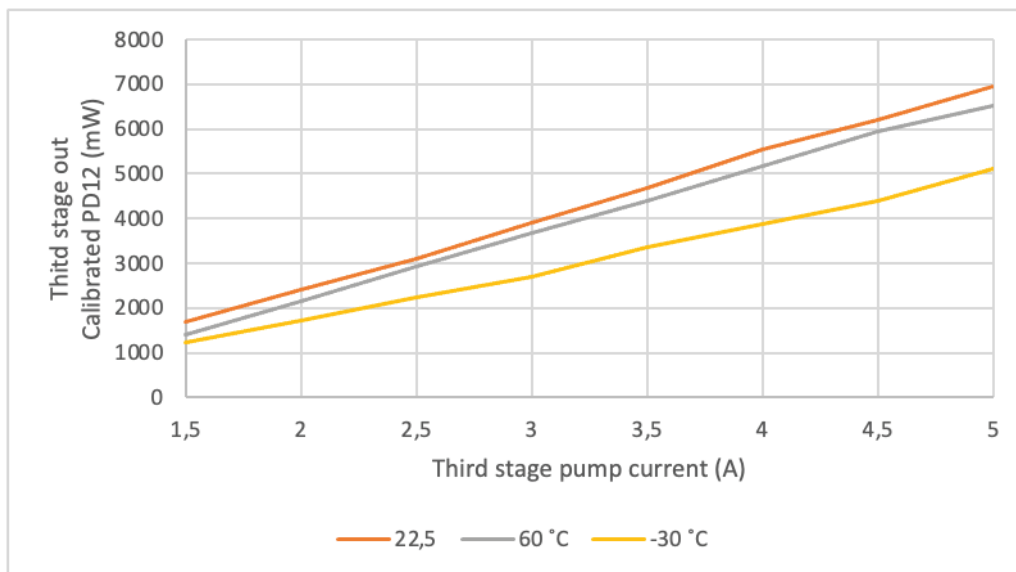


Figure 15. FMC third stage output versus pump current for 3 temperatures. The first stage is operated with a pump current of 350 mA and the second stage pump at 3,1 A.

For the active cycle, the amplifier was powered up by setting the first stage current to 350 mA, the second stage current to 3,1 A and the third stage current to 4.2 A. The input power is 3 mW. The TVAC chamber temperature was then cycled and unit monitors were recorded. The cycle has temperature plateaus to allows the unit to stabilize for a more precise measurement at that temperature. There is a lag between the cold plate in the chamber change temperature and the unit temperature, and in particular the pump temperature, as they heat up the unit.

The active temperature cycle of FMC is present in Figure 16. One can see the amplifier output in maximum between 15 °C and 25 °C, and shows a minimum at 60 °C and another deeper minimum at -30 °C. This is in perfect accordance with the measurement presented in previous sections.

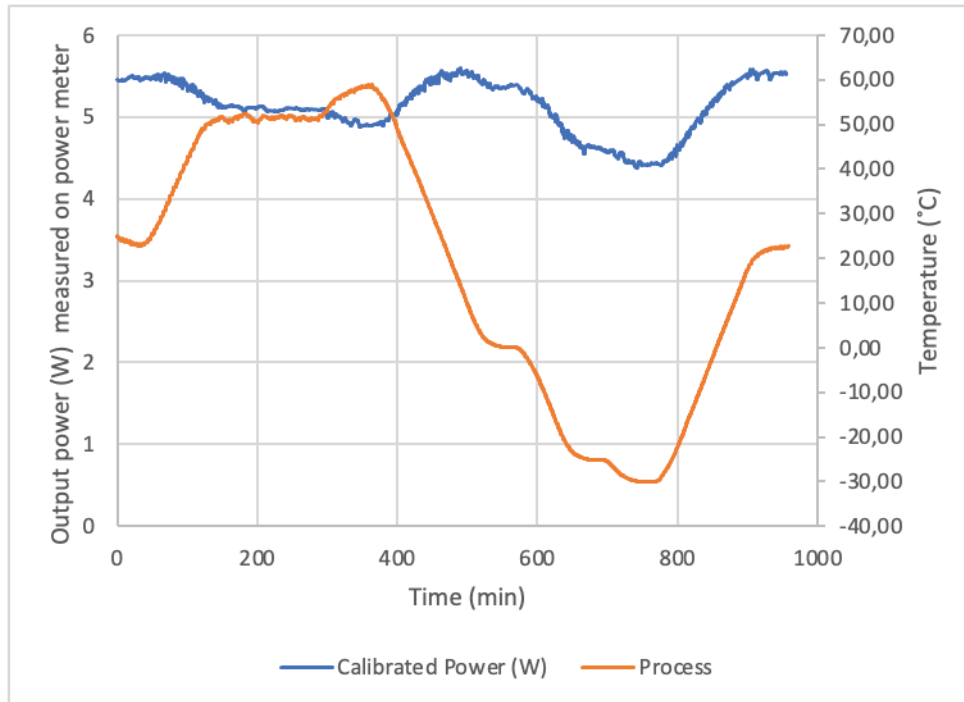


Figure 16. Active cycle of FMA. The process curve is the temperature of the cold plate of the TVAC chamber. The output of the unit is measured by an external power meter.

During the cycle, all the stages and back reflection monitors are recorded. The results can be extracted for each monitor. Instead of being plotted as a function of time, the next graphs show the calibrated monitor powers as a function of temperature.

Figure 17 show the first stage output, monitored by PD1 and PD2. The maximum output power of the first stage is between -15 °C and 0°C. From that point, the power slowly degrades toward the high temperature to about half the maximum value at 60°C. Below - 20°C, we clearly see the effect of shift of the pump off the stabilizing grating as the output drop dramatically from 22 mW to 4 mW. The hysteresis is simply due to the thermal mass of the unit and the lag caused by it during temperature change. The unit is warmer as the temperature goes down and colder as the temperature goes up. This reflects on the temperature of the pump and its absorption.

Figure 18 shows the second stage output, monitored by PD3 and PD4. Unlike the single-mode grating stabilized pump, end because of the long gain fiber, the second stage output is much less affect at cold temperature. The maximum is at -10°C, and is less than 20% below at -30 °C. At high temperature, the loss of efficiency of the pumps has the same effect as in the first stage. The power is 50% down at 60 °C.

Figure 19 shows the backward propagation power from stage 2 and 3. The second stage monitor PD7 and PD8 measures an increase in power as the temperature drops below -20 °C. This exactly correlates with the decrease of the output of the first stage. This can be directly explained by an increase of the backward propagating ASE created by the lower input signal. The backward propagating of stage 3 is very small, showing very little ASE.

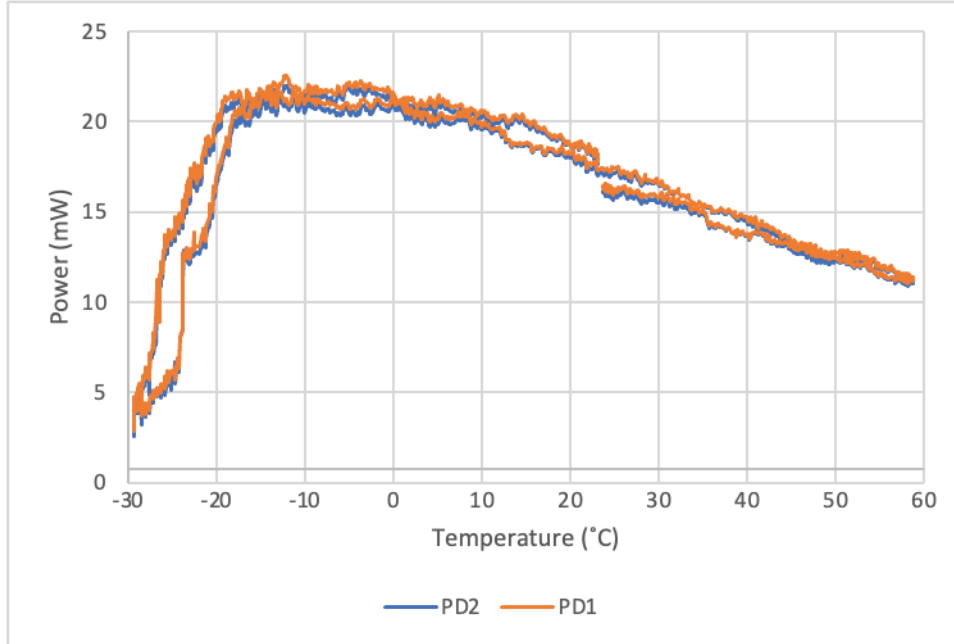


Figure 17. First stage output for a 350 mA pump current during active cycling of FMA .

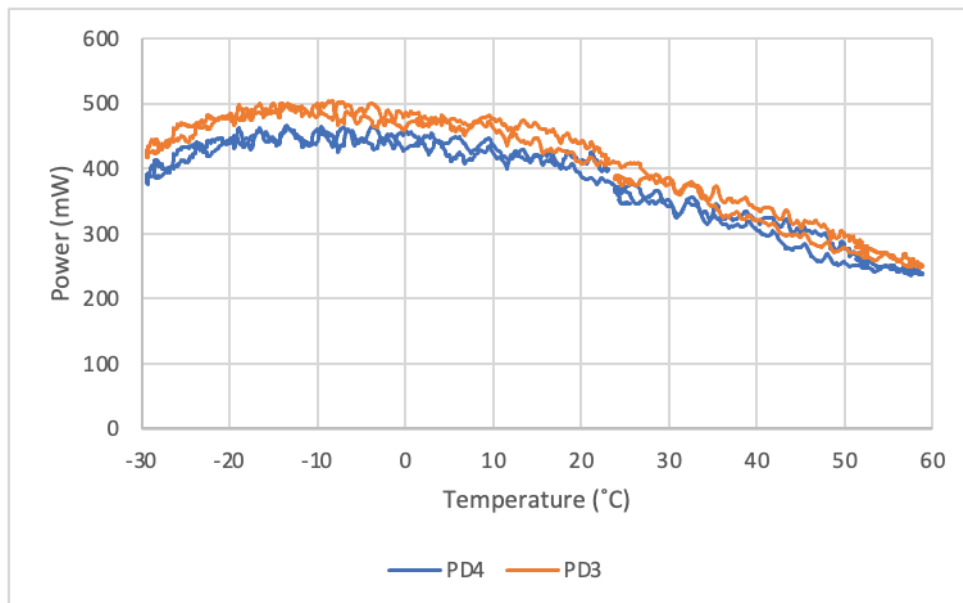


Figure 18. Second stage output for a 3.1 A pump current during active cycling of FMA. First stage pump current is 350 mA.

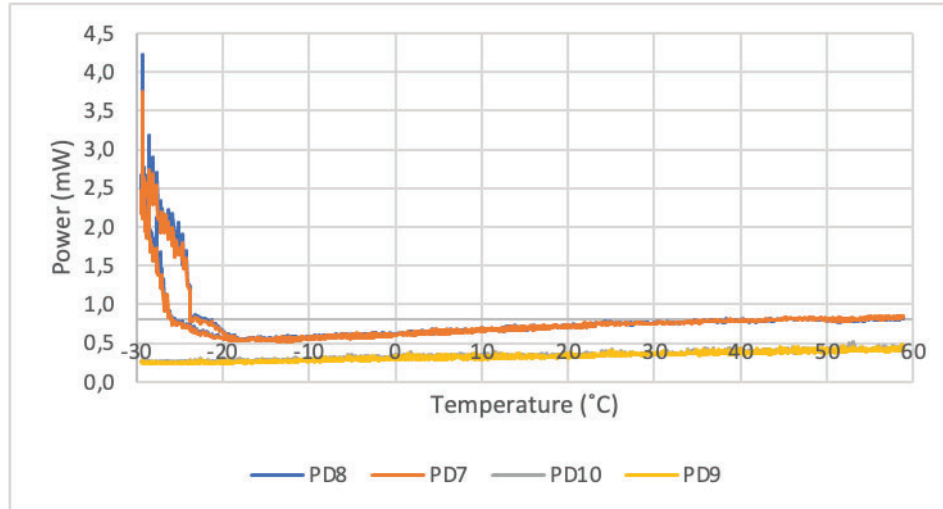


Figure 19. Back reflection monitors during active cycling of FMA. PD7 and PD8 monitor the back-propagating power from stage 2 and PD9 and PD10 from stage 3.

Figure 20 shows the output power of the amplifier as a function of temperature, during the active cycle. The maximum is between 15°C and 25°C at 5.55 W. It also shows a gradual 20% decrease toward the cold temperature without any sign of the first stage degradation at -20°C. The decrease toward high temperature is 10%. Thus, even if the pump wavelength shift and the pump efficiency change, the amplifier operates smoothly over the temperature range.

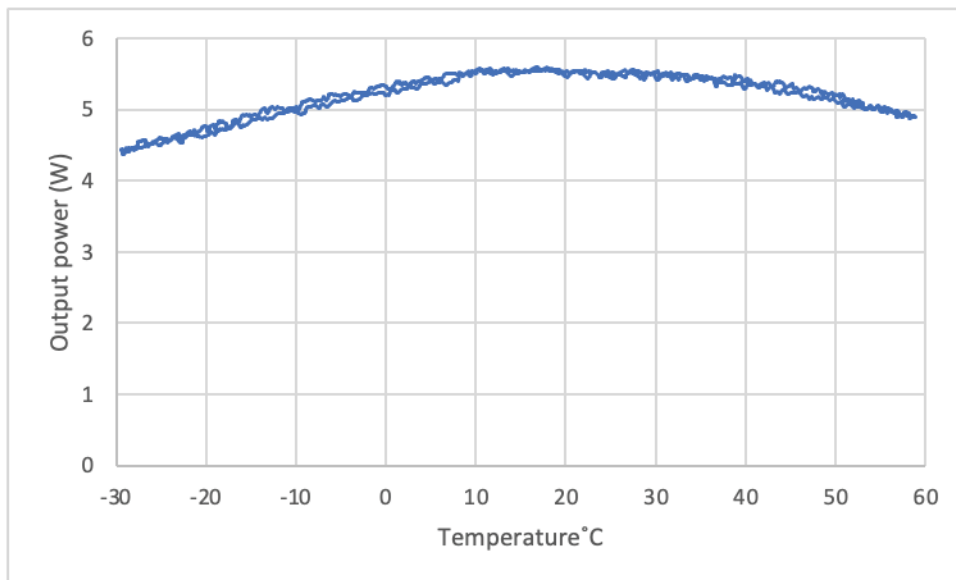


Figure 20. FMA Output power (external power meter) during active cycle.

## 6. CONCLUSION

We have designed and built 1064 nm 6W fiber amplifiers for space applications, with a minimum 5W output over a -35°C to +65°C temperature range. The amplifier is full cold redundancy on the optoelectronics element and has 2 redundant input ports. The input and output fiber are polarization maintaining single-mode fibers and the PER is better than 20 dB. The amplifier is a 3-stage design. A qualification module was built and tested in a TVAC chamber over the full 100 °C temperature range. The module was successfully tested but showed more limited power output at cold

temperature within the 5.3A maximum current requirement. The module is able to reach 6 W for higher currents. The module also passed vibration, micro-vibration, shock and EMC tests. The unit was also exposed to 25 krad radiation over 60 hours. The radiation induced photodarkening was reduced by photobleaching and the resulting analysis estimates lifetime dose of 8 krad would produce a 3% degradation. This is well within the operating margin for a 5W operating power.

After the qualification module, 3 flight modules were built and characterized. Each stage performance was analyzed and found that though the first stage lost efficiency below -20°C, the second stage could compensate this performance and the amplifier operates smoothly over the operating temperature range of -30°C to 60 °C.

Acknowledgements: The authors would like to thank Dr. Nikos Karafolas of ESA for his support.

## REFERENCES

- [1] Hamid Hemmati; “Near-Earth Laser Communications”; Second Edition, Hamid-Hemmati, CRC Press, Taylor & Francis Group, 2021-TPC505124
- [2] Rui Li, Baojun Lin, Yingchun Liu, Mingji Dong, Shuai Zhao; “A Survey on Laser Space Network: Terminals, Links, and Architectures”; IEEE Access, <https://doi.org/10.1109/ACCESS.2022.3162917>
- [3] ESA telecom ARTES 4.0, High Power 1064nm Optical Amplifier, <https://artes.esa.int/projects/high-power-1064nm-optical-amplifier>
- [4] E. Haddad, V. Poenariu, K. Tagziria, W. Shi, C. Chilian, N. Karafolas, I. McKenzie, M. Sotom, M. Aveline, "Comparison of gamma radiation effect on erbium doped fiber amplifiers," Proc. SPIE 10562, International Conference on Space Optics — ICSO 2016, 1056219 (25 September 2017); <https://doi.org/10.1117/12.2296186>
- [5] Emile Haddad, François Gonthier, QiYang Peng, Viorel Poenariu, Kamel Tagziria, Jonathan Lavoie, Piotr Murzionak, Gregory Schinn, Nikos Karafolas, Charlotte Bringer, "10W single-mode PM optical amplifiers in the 1.5 μm for space applications," Proc. SPIE 11180, International Conference on Space Optics — ICSO 2018, 1118035 (12 July 2019); <https://doi.org/10.1117/12.2536032>